

Sb-doping effect on thermal and electrical properties of Ge-rich Ge_{1-x}Sn_x layers

Taisei Iwahashi¹, Masashi Kurosawa^{1,2,3}, Noriyuki Uchida⁴, Yuji Ohishi⁵,
Tatsuro Maeda⁴, Osamu Nakatsuka^{1,6}, and Shigeaki Zaima⁶

¹ Graduate School of Engineering, Nagoya University, Furo-cho, Chikusa-ku, Nagoya 464-8603, Japan

² Institute for Advanced Research, Nagoya University, Furo-cho, Chikusa-ku, Nagoya 464-8601, Japan

³ PRESTO, Japan Science and Technology Agency, 4-1-8, Honcho, Kawaguchi, Saitama 332-0012, Japan

⁴ Nanoelectronics Research Institute, National Institute of Advanced Industrial Science and Technology (AIST),
1-1-1 Higashi, Tsukuba, Ibaraki 305-8568, Japan

⁵ Graduate School of Engineering, Osaka University, Yamadaoka 2-1, Suita, Osaka 565-0871, Japan

⁶ Institute of Materials and Systems for Sustainability, Nagoya University, Furo-cho, Chikusa-ku, Nagoya 464-8603, Japan

Phone: +81-52-789-3817 E-mail: kurosawa@alice.xtal.nagoya-u.ac.jp

Abstract

Thermoelectric properties of undoped and Sb-doped Ge_{1-x}Sn_x ($x = 0-0.06$) layers grown on Si(001) by low-temperature MBE have been firstly demonstrated. Although domain size in an Sb-doped Ge_{0.94}Sn_{0.06} layer was very small (2.3 nm), the layer showed n-type conduction. Correspondingly, a very low thermal conductivity of 1.4 Wm⁻¹K⁻¹, which is almost the same as that for amorphous Si (1–2 Wm⁻¹K⁻¹), has been achieved, leading high-performance thermoelectric generator. The thermoelectric power and its potential will be discussed.

1. Introduction

Ge_{1-x}Sn_x has been studied mainly in the field of group-IV optoelectronics, especially aiming for photoemission [1]. This is because Ge_{1-x}Sn_x turns out to have a direct band gap (less than 0.5 eV) in the infrared region, which values can be tuned through the Sn content x (more than 6–8%). It was theoretically predicted that Ge_{0.92}Sn_{0.08} shows very high hole and electron mobilities due to the small effective masses [2]. The incorporated Sn atom in the Ge matrix should play an important role for the scattering of the phonons related to thermal transport. Therefore, Ge_{1-x}Sn_x has a high potential in simultaneous realization of a high electrical conductivity σ and a low thermal conductivity κ , achieving high-performance thermoelectric generator. However, the thermoelectric property of Ge_{1-x}Sn_x has not been investigated experimentally yet.

It is therefore, in this study, we aim to reveal the thermal and electrical properties of Ge-rich Ge_{1-x}Sn_x ($x = 0-0.06$) layers grown by low-temperature molecular beam epitaxy (LT-MBE). Sb-doping effects in the Ge_{1-x}Sn_x on the thermoelectric properties will also be discussed.

2. Experimental Procedure

The following is the detailed procedure for the formation of Ge_{1-x}Sn_x layers by using a LT-MBE technique. A high resistivity (>1000 Ω cm) (001)-oriented Si substrate was used as the substrates in order to isolate electrically from the substrate. After a wet-chemical cleaning of the substrates, we conducted a heat treatment at 600–850 °C in a vacuum chamber with a base pressure of 10⁻⁷–10⁻⁸ Pa. Subsequently, an undoped Ge_{1-x}Sn_x ($x = 0-0.06$) or Sb-doped Ge_{0.94}Sn_{0.06} layer with the Sb content of 1.0×10²⁰ cm⁻³ was directly grown on the substrate by coevaporating Ge, Sn, and Sb using Knudsen cells. X-ray diffraction two-dimensional reciprocal space mapping (XRD-2DRSM) around the Ge $\bar{2}24$ reciprocal lattice points (a typical result: Fig. 1) revealed that all of the Ge_{1-x}Sn_x layers were

fully epitaxial and strain relaxed; the elliptical diffraction pattern is inclined with both direction of 001 and $\bar{1}10$ suggesting microscopic tilt distribution in the layer. Some of the Sb-doped samples were annealed at various temperatures between 400 and 600 °C for 1 s in a dry N₂ atmosphere.

We used 2ω (Advance Riko, TCN-2 ω) or pico-second thermoreflectance method (PicoTherm, PicoTR) to analyze κ of the Ge_{1-x}Sn_x in the thickness direction.

3. Results and discussion

Lateral correlation length (domain size) caused by microscopic tilt in crystals should affect the thermal conductivity as well as the electrical conductivity in the crystals; thus, we firstly confirmed the crystallographic structures and then compared them with the thermal and electrical properties. The lateral correlation length $\langle L \rangle$ in Ge_{1-x}Sn_x layers was estimated from the peak position (q_x , q_y) and full width at half maximums of the ellipse (Δq_x and Δq_y) in the XRD-2DRSM by using equations:

$$\langle L \rangle = - [1/(\Delta q_x^2 + \Delta q_y^2)^{1/2}] \times [\sin \phi / \cos(\phi + \xi)], \quad \phi = \tan^{-1}(q_x/q_y),$$

$$\text{and } \xi = \tan^{-1}(\Delta q_x/\Delta q_y) [3].$$

Figure 2 shows $\langle L \rangle$ versus κ for various Ge_{1-x}Sn_x layers grown on Si(001) and Ge(001) [4], where the calculated value of κ for various Sn contents and phonon scattering length are also shown for comparison. The $\langle L \rangle$ for undoped Ge_{1-x}Sn_x/Si samples was kept less than 7 nm, resulting in lower κ compared with Ge_{1-x}Sn_x/Ge samples. Specifically, 4.1, 2.3, and 1.9 Wm⁻¹K⁻¹ were obtained for $x=0$, 0.03, and 0.06, respectively. In addition, it is found that an additional reduction in the κ was realized by the Sb doping (see arrow in Fig. 2). The resulting minimum κ for the Sb-doped Ge_{0.94}Sn_{0.06}/Si sample (1.4 Wm⁻¹K⁻¹), which is almost the same as that for amorphous Si (1–2 Wm⁻¹K⁻¹) [5], is about 26% smaller than that for undoped one whose $\langle L \rangle$ value was 2.3 nm. From the results, we roughly estimated number of incorporated atoms in the domains in order to clear a dominant factor reducing the κ . For the undoped Ge_{0.94}Sn_{0.06}/Si sample, there are 17 Sn atoms in the domain; for the Sb-doped Ge_{0.94}Sn_{0.06}/Si sample, there are 15 Sn atoms and 1 Sb atom. The atomic size is near between Sn and Sb; number of the incorporated atoms is almost same between the two samples. Consequently, we infer that the additional reduction of κ by the Sb doping comes mainly from scatterings caused by the domain boundaries not the incorporated atoms in the Ge matrix.

To evaluate electrical activation of Sb atoms, hard X-ray photoelectron spectroscopy (HAXPES) measurements were carried out for Sb-doped Ge_{0.94}Sn_{0.06}/Si samples before and after post annealing. Figure 3(a) shows the Sb3d_{3/2} spectrum

taken for the sample before post annealing. The spectrum was deconvoluted into 3 components related to chemical bonds of oxidized Sb, substitutional Sb (activated), and isolated Sb (not activated). We estimated activated Sb density from the ratios of the area intensity of activated Sb to the area intensity of Ge 3d [Fig. 3(b)]. Here, the electron density extracted from Hall effect measurements is also shown for comparison. In the as-grown sample, the activated Sb density shows a relatively high value of $5.6 \times 10^{19} \text{ cm}^{-3}$, which exceed the solid solubility limit of Sb in Ge ($1.2 \times 10^{19} \text{ cm}^{-3}$) [6]. However, the Hall electron density ($2.6 \times 10^{18} \text{ cm}^{-3}$) was lower than the activated Sb density, suggesting generation of holes in the $\text{Ge}_{1-x}\text{Sn}_x$ layer. We previously reported that holes were generated in undoped $\text{Ge}_{1-x}\text{Sn}_x$ layers ($x = 0-0.058$) epitaxially grown on SOIs [8]. With increasing post-annealing temperature, the activated Sb density decreases and the Hall electron density begins to increase. As a result, the two densities become same value of $1 \times 10^{19} \text{ cm}^{-3}$ after annealing at 600°C . These results clearly indicate that tuning of the post-annealing process for Sb-doped $\text{Ge}_{1-x}\text{Sn}_x$ layers is very important to enhance the electron density.

Finally, we measured Seebeck coefficient S and electrical conductivity σ for various samples (Fig. 4). The power factor ($P=S^2\sigma$) slightly increases up to $\sim 0.14 \text{ mW}\cdot\text{K}^{-2}\cdot\text{m}^{-1}$ after post annealing at 600°C . Unfortunately, because of the low σ , the obtained power is about 1/30 of that for n-type $\text{Bi}_2\text{Te}_3/\text{Bi}_2\text{Te}_{2.83}\text{Se}_{0.17}$ superlattice [9]. It is noted that the σ in $\text{Ge}_{1-x}\text{Sn}_x$ is at least one order lower than expected values from the Irvin curve of n-type Ge [10] and Sb-doped $\text{Ge}_{1-x}\text{Sn}_x$ layers grown on Ge(001) [7]; thus, the present study does not indicate the limitation of n-type $\text{Ge}_{1-x}\text{Sn}_x$.

4. Conclusions

Thermoelectric characterizations of undoped and Sb-doped Ge-rich $\text{Ge}_{1-x}\text{Sn}_x$ ($x = 0-0.06$) layers grown on Si(001) were demonstrated for the first time. The experimental results clearly showed a very low thermal conductivity of $1.4 \text{ Wm}^{-1}\text{K}^{-1}$, although the thermoelectric power is still small ($\sim 0.14 \text{ mW}\cdot\text{K}^{-2}\cdot\text{m}^{-1}$). We believe that continuing efforts open up the possibilities of high quality n-type $\text{Ge}_{1-x}\text{Sn}_x$ essential for new group-IV thin-film thermoelectric devices.

Acknowledgements

The authors wish to thank Dr. Eiji Ikenaga of JASRI for help with the synchrotron radiation experiments. The HAXPES measurements were carried out at BL47XU in Spring-8 with the approval of JASRI (Proposal No. 2016B0109). This work was partially supported by Grants-in-Aid for Scientific Research (S) (Grant No. 26220605) and Young Scientists (A) (Grant No. 17H04919) from JSPS in Japan and PRESTO (Grant No. JPMJPR15R2) from JST in Japan.

References

- [1] Wirths *et al.*, Nature Photonics **9**, 88 (2015).
- [2] Sau and Cohen, Phys. Rev. B **75**, 045208 (2007).
- [3] P. F. Fewster, *X-ray Scattering from Semiconductors*, 2nd ed., (Imperial College Press, 2000), p. 266.
- [4] M. Kurosawa *et al.*, "Thermophysical characterizations of $\text{Ge}_{1-x}\text{Sn}_x$ epitaxial layers aiming for thermoelectric device," 9th International Conference on Silicon Epitaxy and Heterostructures (ICSI-9), Montreal, Canada, 4.4.1, May 21, (2015).
- [5] D. G. Cahill *et al.*, J. Vac. Sci. Technol. A **7**, 1259 (1989).
- [6] C. Claeys *et al.*, *Germanium-Based Technologies: From Material to Devices*, 1st ed., (Elsevier, 2007), p. 86.
- [7] J. Jeon *et al.*, JJAP **55**, 04EB13 (2016).
- [8] O. Nakatsuka *et al.*, JJAP **49**, 04DA10 (2010).
- [9] R. Venkatasubramanian *et al.*, Nature **413**, 597 (2001).
- [10] S. M. Sze, *Physics of Semiconductor Devices*, 2nd ed., (Wiley, 1981), p. 33.

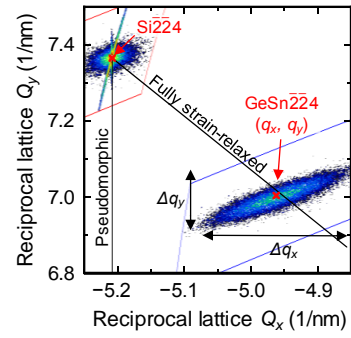


Figure 1 XRD-2DRSM obtained from the Sb-doped $\text{Ge}_{0.96}\text{Sn}_{0.06}$ layer grown on Si(001) substrate.

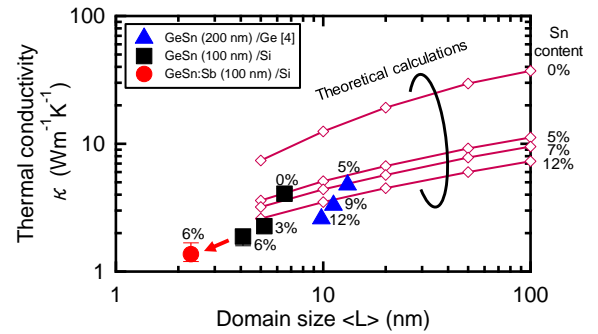


Figure 2 Thermal conductivity κ vs lateral correlation length (domain size) $\langle L \rangle$ for undoped and Sb-doped $\text{Ge}_{1-x}\text{Sn}_x$ layers grown on Si(001) or Ge(001). Theoretical calculated values are also shown for comparison.

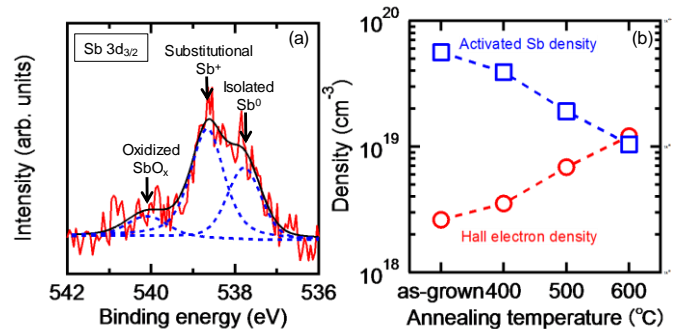


Figure 3 (a) Sb $3d_{3/2}$ core level spectrum taken for the Sb-doped $\text{Ge}_{0.94}\text{Sn}_{0.06}/\text{Si}$ sample before post annealing. (b) The post-annealing temperature dependence of the activated Sb density and Hall electron density for the Sb-doped sample.

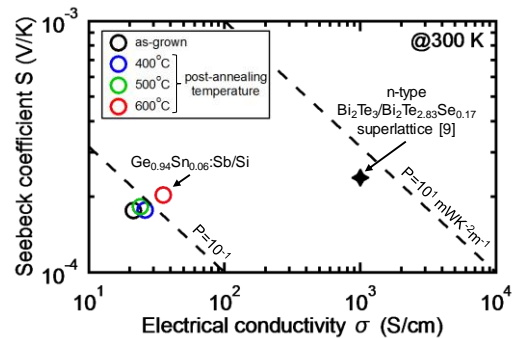


Figure 4 Seebeck coefficient S vs electrical conductivity σ at for Sb-doped $\text{Ge}_{1-x}\text{Sn}_x/\text{Si}$ samples before and after post annealing. The measurement temperature was 300 K.